Water Research 155 (2019) 310–319

Contents lists available at ScienceDirect

Water Research

journal homepage: www.elsevier.com/locate/watres

Insight into the roles of packing carriers and ultrasonication in anaerobic side-stream reactor coupled membrane bioreactors: Sludge reduction performance and mechanism

Yue Zheng [a, 1], Cheng Cheng [a, c, 1], Zhen Zhou [a, b, *], Hongjian Pang [a], Liuyu Chen [a], Lu-Man Jiang [a]

[a] College of Environmental and Chemical Engineering, Shanghai University of Electric Power, Shanghai, 200090, China
[b] Shanghai Institute of Pollution Control and Ecological Security, Shanghai, 200092, China
[c] State Key Laboratory of Pollution Control and Resource Reuse, School of the Environment, Nanjing University, Nanjing, 210023, Jiangsu, PR China

ARTICLE INFO

Article history:
Received 2 December 2018
Received in revised form
20 February 2019
Accepted 22 February 2019
Available online 26 February 2019

Keywords:
Sludge reduction
Anaerobic side-stream reactor
Carrier
Ultrasonication
Microbial community

ABSTRACT

The sludge *in situ* reduction process by inserting an anaerobic side-stream reactor (ASSR) in a sludge return line provides a cost-effective approach to reduce sludge production in activated sludge systems. In this study, four pilot-scale membrane bioreactors (MBRs), including an AO-MBR for control, ASSR coupled MBR (ASSR-MBR), a MBR with ASSR packed with carriers (AP-MBR) and an AP-MBR with part of sludge ultrasonicated before fed into ASSR (AUP-MBR) were operated in parallel to investigate enhancing effects of ultrasonication and packing carriers on sludge reduction and pollutants removal performance under both normal and low temperature. Low temperature showed negligible impact on COD removal, deteriorated NH_4^+–N and TN removal from 98.3% to 69.7% at 21.6 °C to 92.5% and 48.8% at 2.6 °C, and decreased sludge reduction efficiency (SRE) in ASSR-MBR. Packing carriers and ultrasonication both enhanced sludge reduction, especially under low temperature with SRE values increased from 8.2% of ASSR-MBR to 17.1% of AP-MBR and 32.6% of AUP-MBR at 4.5 ± 2.5 °C. Packing carriers and ultrasonication increased cell rupture by 11.1% and 14.5% in aerobic MBR, enhanced protease activity in ASSR by 60.0% and 116.3%, and reduced ATP content for heterotrophic metabolism by 31.4% and 7.3%, respectively. *MiSeq* sequencing results showed that packing carriers enriched hydrolytic bacteria (*Terrimonas, Dechloromonas* and *Woodsholea*), slow growers (*Sulfuritalea*, *Thauera* and *Azospira*) and predatory bacteria (*Bdellovibrio* and *norank_Saprospiraceae*), while ultrasonication further enriched hydrolytic bacteria (*norank_Saccharibacteria* and *Ferruginibacter*). Packing carriers is more cost-effective than ultrasonication to enhance sludge reduction by partial damage to bacterial cells and promoting better interaction between bacteria, enzymes and substrates to favor particles hydrolysis.

1. Introduction

As an inevitable by-product of wastewater treatment plants (WWTPs), waste activated sludge (WAS) requires complicated processes for stabilization, dewatering and disposal, accounting for 25%–65% of the total operation cost of WWTPs (Saby et al., 2003; Zhou et al., 2015). Many sludge *in situ* reduction (SIR) approaches have been proposed as a cost-efficient way to decrease WAS production within the biological wastewater treatment process (Niu et al., 2016b). Biological process with an anaerobic side-stream reactor (ASSR) placed in the sludge return loop and its derivation, oxic-settling-anaerobic process, have been intensively studied in lab, pilot and full-scale systems (Cheng et al., 2017; Troiani et al., 2011; Velho et al., 2016). Effects of oxidation-reduction potential (ORP) level (Saby et al., 2003; Wang et al., 2015), hydraulic retention time (HRT) (Jiang et al., 2018; Semblante et al., 2016; Ye et al., 2008) and side-stream ratio (Cheng et al., 2017) on sludge reduction performance has been investigated to optimize operational parameters and identify the main mechanism governing sludge reduction. Nevertheless, wide fluctuations in sludge reduction efficiency (SRE) of ASSR (0.2%–66%) were observed in literature

* Corresponding author. College of Environmental and Chemical Engineering, Shanghai University of Electric Power, Shanghai, 200090, China.
E-mail address: zhouzhen@shiep.edu.cn (Z. Zhou).
[1] Both authors contributed equally to this manuscript.

https://doi.org/10.1016/j.watres.2019.02.039
0043-1354/

(Foladori et al., 2015; Pang et al., 2018) with a long HRT of ASSR (6–7 h) comparable to the main stream. Therefore, exploring enhancement strategies for ASSR to ensure high and stable SRE are important for its practical application.

Packing carriers was proved to effectively improve SRE of ASSR by enriching functional bacteria and accelerating sludge reduction with more abundant microbial communities and longer microbial food chains (Cheng et al., 2018b). Physicochemical pretreatments aiming at destructing sludge flocs and disrupting cells are also an alternative. Of all physicochemical options, ultrasonication shows advantages over chemical oxidation for generating no hazardous residue in sludge and promoting enzymatic activity at low intensity (Foladori et al., 2010). Ultrasonication also improves sludge disintegration and cell membrane permeability (Xie et al., 2009) because the sudden collapse of cavitation microbubbles generated around the sonotrode upon reaching critical dimension lead to a large amount of energy released as heat, pressure, turbulence and intensive shearing force (Romero-Pareja et al., 2017). So far ultrasonication has been successfully applied in pretreatment for sludge reduction and anaerobic digestion (Romero-Pareja et al., 2017; Yang et al., 2012), and detailed techno-economic investigation is required for the combination of ultrasonication with sludge reduction.

In this study, ASSR were coupled with membrane bioreactors (MBR) to construct a process with efficient pollutants removal and sludge reduction because MBR showed advantages of efficient solid separation, small footprint, enriching nitrifiers, etc (Cheng et al., 2017; Sepehri and Sarrafzadeh, 2018). Four pilot-scale MBRs, including an anaerobic-oxic MBR (AO-MBR) for control, an MBR with ASSR (A-MBR), a MBR with ASSR packed with carriers (AP-MBR) and an AP-MBR with part of sludge ultrasonicated before fed into ASSR (AUP-MBR) (Fig. 1) were operated in parallel to investigate enhancing effects of ultrasonication and packing carriers on sludge reduction and pollutants removal performance. Effect of temperature was also evaluated. Analyses on cell integrity, total adenosine triphosphate (ATP) and protease activity were conducted to reveal possible sludge reduction mechanisms. *MiSeq* sequencing was applied to correlate microbial community structure and population composition with process performance. The results are expected to clarify enhancement mechanisms of ultrasonication and carriers on performance of ASSR.

2. Materials and methods

2.1. Batch tests for sludge ultrasonication and hydrolysis

A series of batch tests were conducted with sludge pretreated by ultrasonication and then hydrolyzed through cell lysis-cryptic growth. The WAS used in this study was collected from RAS line of the Dongqu WWTP (Shanghai, China) with an anaerobic-anoxic-oxic (AAO) process. The main characteristics of WAS sample were as follows: pH of 7.88 ± 0.05, mixed liquor suspended solid (MLSS) of 4.70 ± 0.10 g/L, mixed liquor volatile suspended solid (MLVSS) of 3.33 ± 0.23 g/L and filtrate total Kjeldahl nitrogen (TKN) of 1.36 ± 0.13 mg/L.

A 200 mL WAS sample was pretreated by a JY98-IIIN ultrasonic cell disruptor (Ningbo Xinzhi, China) with energy density of 0 (raw sludge), 0.1, 0.2, 0.4 and 0.8 W/mL for 10 min, and ultrasonication time of 0, 5, 10, 15 and 20 min at energy density of 0.2 W/mL. Then the pretreated sludge was mixed with 1.8 L of sludge collected from ASSR. All the batch reactors were continuously stirred at 200 rpm for 24 h at 20.0 ± 0.1 °C. A 100 mL sludge sample was withdrawn at 0, 0.5, 1, 2, 4, 8, 12 and 24 h, and filtered through 0.45 μm vinyl cellulose membrane to analyze sludge concentration variation and TKN release in the hydrolysis process.

2.2. Hydrolysis kinetics for sludge after ultrasonication

The hydrolysis rate of sludge after ultrasonic disintegration follows a first-order kinetic equation shown in Eq. (1)

$$dX/dt = -k(X - X_I) \quad (1)$$

where X and X_I are concentrations of hydrolysable sludge and sludge inert to hydrolysis, mg/L; k is the first-order kinetic constant, d^{-1}. Integration of Eq. (1) gives,

$$X = (X_0 - X_I)e^{-kt} + X_I \quad (2)$$

where X_0 is the initial sludge concentration, mg/L. The dissociation of extracellular polymeric substances (EPS) and the release of intracellular substances are accompanied by sludge disintegration in the hydrolysis process, and manifested by the increase of soluble COD, nitrogen, phosphorus, etc. Assume a certain substrate is evenly distributed in the sludge, then its released concentration in the hydrolysis process is proportional to the concentration of disintegrated sludge, namely

$$\frac{dS_i}{dt} = -\alpha_i \frac{dX}{dt} = \alpha_i kX \quad (3)$$

where S_i is the concentration of substrate i, mg/L;α_i is the proportion of substrate i in the sludge. Substituting Eq. (2) into Eq. (3) gives:

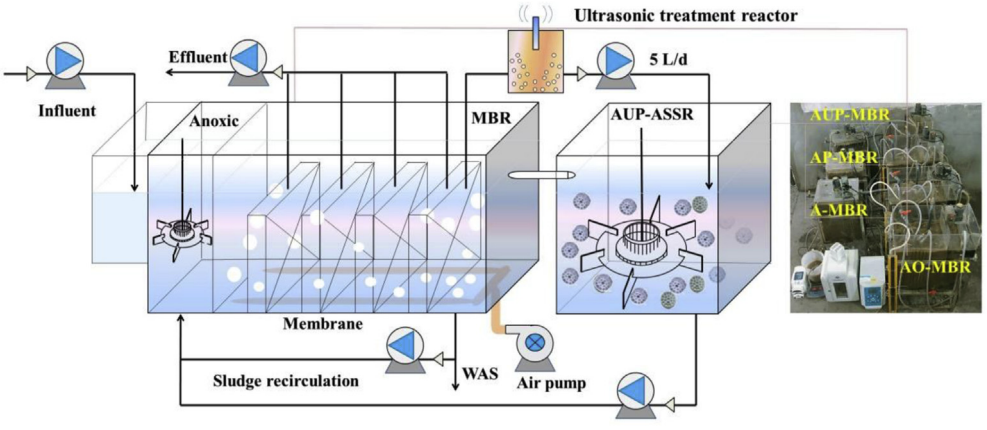

Fig. 1. Schematic diagram of AO-MBR process coupled carriers enhanced ASSR and ultrasonic treatment for sludge reduction.

$$S_i - S_{i,0} = \alpha_i(X_0 - X_I)\left(1 - e^{-kt}\right) \quad (4)$$

where $S_{i,0}$ is the initial concentration of substrate *i*, mg/L.

2.3. Pilot-scale experimental system and operating conditions

Four pilot-scale MBRs, including an AO-MBR and three ASSR-MBRs (A-MBR, AP-MBR and AUP-MBR) (Fig. 1), were operated in parallel for 141 days in Dongqu WWTP (Shanghai, China) and fed with wastewater from the grit chamber. Effective volumes of anoxic tank, MBR and ASSR were 16.7, 50 and 50 L, respectively. The anoxic tank and ASSR were equipped with an agitator to maintain sludge suspended. In each MBR, flat-sheet PVDF membrane with an average pore size of 0.2 μm and a total effective filtration area of 0.25 m^2 was mounted vertically. Each MBR system consisted of an air diffuser, a pressure gauge and three peristaltic pumps that had been described in a previous paper (Cheng et al., 2017). To mitigate membrane fouling, intermittent filtration mode with 2 min pause for every 10 min suction was employed. Mechanical cleaning and in-place chemical cleaning with 0.5% (v/v) NaClO solution were conducted for membranes when the trans-membrane pressure exceeded 25 kPa. In AP-MBR and AUP-MBR system, the ASSR was packed with cylindrical-shaped polyethylene carrier elements (specific density of 0.96–0.98 g/cm^3), SPR-1, with filling rate of 15%. The packing cylinders are 24 mm in diameter and 12 mm in height with a cross inside the cylinder and longitudinal stripes on the outside.

Concentrations of dissolved oxygen (DO) in the four MBRs were all maintained at 4.0–5.0 mg/L. The four MBRs were operated without temperature control, and thus went through three stages according to temperature variation: Stage I at 21.6 ± 4.9 °C for the first 64 days, Stage II at 6.5 ± 1.7 °C from Day 65–120, Stage III at 2.6 ± 1.4 °C for the last 21 days. The wastewater was continuously fed into the four MBRs with membrane flux of 15 L/(m^2·h) at Stage I and 12 L/(m^2·h) at Stage II and III to prevent severe membrane fouling. The mixed liquor recirculation ratios were all controlled at 250% for the four MBRs, and 40% of the recirculation was passed through the ASSR in the three ASSR-MBRs. In AUP-MBR, sludge with flow rate of 5 L/d was taken from the 40% recirculation and fed into ultrasonic treatment reactor (UTR) for ultrasonication with energy density of 0.2 W/mL for 10 min obtained by batch tests before discharged to ASSR. The concentration of MLSS in each MBR was maintained at 6500 mg/L by discharging WAS from the MBR.

2.4. Analytical methods

2.4.1. Cell integrity analysis

Flow cytometry (FCM) for the rapid quantification of intact or ruptured cells in bacterial population has been applied in various studies for multi-parametric and single-cell analysis (Foladori et al., 2015; Han et al., 2016). Cell membrane integrity tests were performed by a double staining method using calcein-AM (CAM) (for live cells) and propidium iodide (PI) (for dead cells) (Han et al., 2017). Samples collected from MBR, UTR and ASSR were centrifugated at 8000 g for 5 min. After discarding supernatant, the remaining pellet was washed by HEPES buffer prior to being re-suspended and diluted for 100 times in 15.4 mM NaCl solution. Then the bacterial suspension was subject to ultrasonication with a power density of 1.3 W/mL for 2 min to disperse the microbial cells. Then the suspension was diluted to a final concentration of 2 mg/L by pre-determined CAM and PI, and incubated for 30 min in the dark. As a consequence, intact and ruptured bacteria emit green and red fluorescence, respectively. FCM (Accuri C6, Bection Dickinson, USA) was then used to determine cell integrity at a flow rate of 10 μL/min. Fluorescence emission of live and dead cells was detected at the FL1 channel (530 nm) and FL2 channel (585 nm), respectively. Data acquisition gates were set on green and red fluorescence distribution to eliminate non-bacterial particles and debris. At least 10,000 cells were analyzed for each sample in a few minutes, providing good statistical data.

2.4.2. ATP and protease activity determination

ATP and protease activity were measured for samples collected from MBR, UTR and ASSR by using the ELISA kit (Shanghai Hengyuan Biotech). The sludge samples were diluted for 5 times and incubated on the enzyme plate at 37 °C for 30 min. The cycle for discarding the supernatant, injecting washing solution and incubation for 30 min was repeated for 5 times. After that, the enzyme standard reagent was added and incubated for 30 min 50 μL reagents A and B from the ELISA kit were added into the sample sequentially and mix at 37 °C for 15 min in the dark. Finally, 50 μL termination agent was added to stop the reaction and the absorbance of the samples was measured by Labsystems Multiskan MS at 450 nm in 15 min.

2.4.3. Microbial community analysis

Ten sludge samples were gathered from three ASSRs ($ASSR_A$, $ASSR_{AP}$ and $ASSR_{AUP}$), four MBRs (AO-MBR, MBR_A, MBR_{AP} and MBR_{AUP}), UTR and sludge attached on the surface of carriers in $ASSR_{AP}$ and $ASSR_{AUP}$ (P_{AP} and P_{AUP}) on Day 138 for *MiSeq* sequencing. Deoxyribonucleic acid extraction, polymerase chain reaction amplifications and amplicons purification were conducted in accordance with the reported methods (Cheng et al., 2017). After purification, amplicons from the samples were sequenced using the *Illumina-MiSeq* platform (Shanghai Majorbio Bio-Pharm Technology, China). Finally, more than 32943 high-quality 16S rRNA sequences were produced, and then normalized to 32943 by the sub.sample command of Mothur program for fairly comparison samples at the same sequencing depth. Then the 16S rRNA sequences were clustered into operational taxonomic units (OTUs) with an average length of 440 bp by setting a 3% distance limit (α). Based on the cluster information, Chao, Ace, Shannon, Simpson and Good's Coverage indices were calculated according to our previous study (Zhou et al., 2015).

2.4.4. Analytical methods of other items

Chemical oxygen demand (COD), ammonium nitrogen (NH_4^+–N), nitrate nitrogen (NO_3–N), total nitrogen (TN) and alkalinity in the influent, effluent and mixed liquor filtrate were analyzed every two days according to standard methods (Chinese NEPA, 2012). MLSS and MLVSS were measured every day. ORP, DO and pH values were monitored using an HQ30d portable meter (Hach, USA). Three-dimensional excitation-emission matrix fluorescence spectra were measured using a RF-5301pc fluorospectrophotometer (Shimadzu, Japan), and decomposed by parallel factor (PARAFAC) analysis in MATLAB R2013a (Mathworks, USA) using the DOM Fluor (Niu et al., 2016b). The ammonium uptake rate (AUR) was measured according to Sepehri and Sarrafzadeh (2018) at the last day of Stage I and III under the regulated temperature of 21.6 and 2.6 °C, respectively.

2.5. Statistic and calculation methods

Differences of pollutants in the effluent were compared by one-way factor analysis of variance (ANOVA) using Office Excel 2010 (Microsoft, USA). The observed sludge yield (Y_{obs}, g SS/g COD) was calculated according to the reported methods (Pang et al., 2018).

$$Y_{obs} = \frac{\sum \Delta X_i V_i + \sum Q_w X_w \Delta t}{\sum Q_i (S_0 - S_e)\Delta t} \quad (5)$$

where ΔX_i is the varied sludge concentration in reactor i, mg/L; Δt is duration of the operation period, d; V_i is the volume of reactor i, L; Q_w is flow rate of WAS, L/d; X_w is sludge concentration in WAS, mg/L; S_0 and S_e is substrate concentration of influent and effluent, respectively, mg COD/L. For the AUP-MBR, the effect of ultrasonic treatment on sludge should be deducted, and the Y_{obs} was calculated as Eq. (6),

$$Y_{obs} = \frac{\sum \Delta X_i V_i + \sum Q_w X_w \Delta t + Q_u \Delta X_u}{\sum Q_i (S_0 - S_e)\Delta t} \quad (6)$$

where Q_u is the flow rate of ultrasonication sludge, L/d; ΔX_u is the reduced sludge concentration after ultrasonication in AUP-MBR, mg/L. The sludge decay coefficient (K_d) of ASSR tank was calculated according to Jiang et al. (2018).

3. Results and discussion

3.1. Batch tests for ultrasonic condition optimization

Fig. 2 shows variations of MLSS and TKN of PASSR sludge treated under different ultrasonic energy densities and times. Ultrasonication disintegrated sludge, and resulted in lower MLSS (Fig. 2a) and smaller particle size (Table 1) than that without pretreatment, which accelerated sludge hydrolysis and release of intracellular compounds (e.g. TKN). For raw sludge, sludge hydrolysis (Fig. 2a and c) is synchronized to TKN release, and both tended to a constant level at about 12 h, while the hydrolysis of ultrasonicated sludge was completed at 6–8 h. The attacks of large cavitation bubbles and powerful hydrodynamic shear force created by the low frequency ultrasound on sludge particles (Van de Moortel et al., 2017) lead to the destruction of cell wall of microorganism, further resulting in not only the release of intracellular compounds but also breakage of aggregates, flocs and maybe cells.

Variations of MLSS and TKN in supernatant with time under different ultrasonic energy densities and times were fitted by Eq. (2) and Eq. (4), respectively, and the results are shown in Table 1. The high coefficients of determination in the fit curve lend credibility to the first-order kinetics. With ultrasonic energy density increasing from 0 to 0.8 W/mL, first-order kinetic constants of MLSS disintegration (k_1) and TKN release (k_2) both increased firstly and then decreased, indicating peak values of 0.349 and 0.660 d^{-1} at 0.2 W/mL, respectively. The same trends of k_1 and k_2 varied with ultrasonication time are also observed with peak values of 0.370 and 0.504 d^{-1} observed at 10 min, respectively. The results indicated that low-intensity ultrasound was more efficient in solubilizing activated sludge and disrupting the sludge floc (Foladori et al., 2010). The higher value of k_2 than k_1 indicated that the rate TKN release was higher than that of solid disintegration, and it was attributed to the uneven distribution of proteins, which were mainly distributed in TB-EPS fraction, a small fraction in slime EPS and very low in LB-EPS (Niu et al., 2016a). In addition, the α_i reached the highest value of 10.58 when the sludge was pretreated under energy density of 0.2 W/mL and 5.16 when the ultrasonic time was 10 min, respectively.

Changes of k and α_i were both firstly increased to the maxima and then gradually decreased with energy density ranged from 0 to 0.8 W/mL and ultrasonic time prolonged from 0 to 20 min. The results can be explained that low-strength and/or short-time ultrasonication elevated biosynthesis of hydrolytic enzymes and facilitated their secretion caused by the disruption of cell wall, and increased activities of the enzymes led to proportional increase of hydrolysis rates (Cho et al., 2017). The microorganisms were damaged gradually by ultrasound although microbial activity still increased due to further improvement in mass transfer, up to a point where further ultrasonic cavitation damaged the cells and

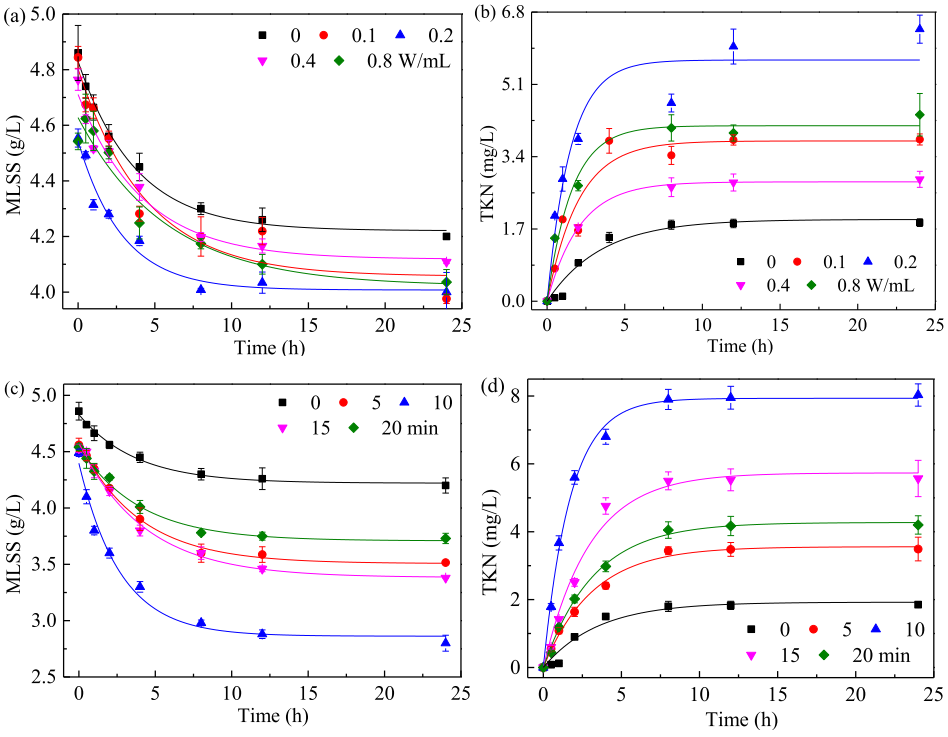

Fig. 2. Sludge disintegration and TKN release during hydrolysis in a PASSR tank after pretreatment under different ultrasonic energy densities and ultrasonication times.

Table 1
Fitting results of sludge disintegration and TKN release during hydrolysis after ultrasonication by first-order kinetic model.

		Particle size (μm)	MLSS				TKN		
			k_1/d^{-1}	X_0	C	R^2	k_2/d^{-1}	α_i	R^2
Ultrasonic energy density (W/mL)	0	56.6 ± 1.6	0.268	4.83	4.22	0.759	0.287	3.16	0.950
	0.1	51.1 ± 2.3	0.227	4.80	4.06	0.931	0.491	5.05	0.923
	0.2	48.4 ± 1.0	0.349	4.54	4.01	0.958	0.660	10.58	0.926
	0.4	36.9 ± 2.2	0.236	4.71	4.12	0.964	0.478	4.74	0.998
	0.8	36.8 ± 2.9	0.174	4.63	4.02	0.927	0.628	6.80	0.996
Ultrasonic time (min)	5	51.7 ± 1.6	0.252	4.58	3.51	0.995	0.385	3.53	0.996
	10	48.4 ± 1.0	0.370	4.40	2.86	0.980	0.504	3.86	0.974
	15	24.9 ± 0.7	0.232	4.58	3.38	0.991	0.242	3.63	0.998
	20	22.3 ± 0.9	0.252	4.54	3.71	0.988	0.375	3.66	0.984

sludge activity decreased drastically (Huan et al., 2009). Therefore, sludge was ultrasonicated at 0.2 W/mL for 10 min, and then pumped to PASSR for posterior hydrolysis for 6.0 h.

3.2. Process performance during long-term experiment

3.2.1. Pollutant removal

After microbial acclimation period, the four systems were continuously operated for 141 days. The pollutant removal performance and regression lines of biomass production were illustrated in Fig. 3. The pH value and alkalinity of influent wastewater were 7.80 ± 0.14 and 346.1 ± 5.6 mg $CaCO_3$/L, respectively, and the mass ratio of alkalinity to NH_4^+–N was 17.13 g $CaCO_3$/g N, which is adequate to buffer alkalinity consumption of nitrification (Sepehri and Sarrafzadeh, 2018). In stage I, the four systems were almost equally effective in the removal of COD (90.3–91.3%) and NH_4^+–N (97.6–98.6%). The one-way ANOVA ($\alpha = 0.05$) results showed that COD removal and nitrification of AO-MBR were not impaired after inserting ASSRs. Compared to AO-MBR with TN removal of 41.0%, A-MBR, AP-MBR and AUP-MBR achieved higher efficiency of 59.9%, 60.9% and 69.6%, respectively. ANOVA ($\alpha = 0.05$) showed that there was significant difference among TN concentrations in the effluents of the four MBRs.

In Stage II and III under low temperature, COD removal was not affected, and it was in agreement with Arévalo et al. (2014), who reported that no significant effect was observed on COD removal with temperature varied from 9 to 33 °C. AUR values of sludge in AO-MBR, A-MBR, AP-MBR and AUP-MBR were 1.14 ± 0.09, 0.71 ± 0.01, 0.86 ± 0.04 and 0.81 ± 0.02 mg N/(g SS·h) in stage I at 21.6 °C, and reduced to 0.15 ± 0.01, 0.21 ± 0.02, 0.25 ± 0.02 and 0.39 ± 0.01 mg N/(g SS·h) in stage III at 2.6 °C, respectively. The results indicated that low temperature in Stage II and III deteriorated NH_4^+–N removal and thus TN removal because nitrification is the premise of denitrification (Hoang et al., 2014). Concentrations of NH_4^+–N and TN in the effluent were increased rapidly to 5.27–11.49 and 15.72–19.30 mg/L in Stage II even though HRT was prolonged from 6.7 to 8.3 h by reducing membrane flux. In stage III, NH_4^+–N and TN removal was remarkably improved compared to

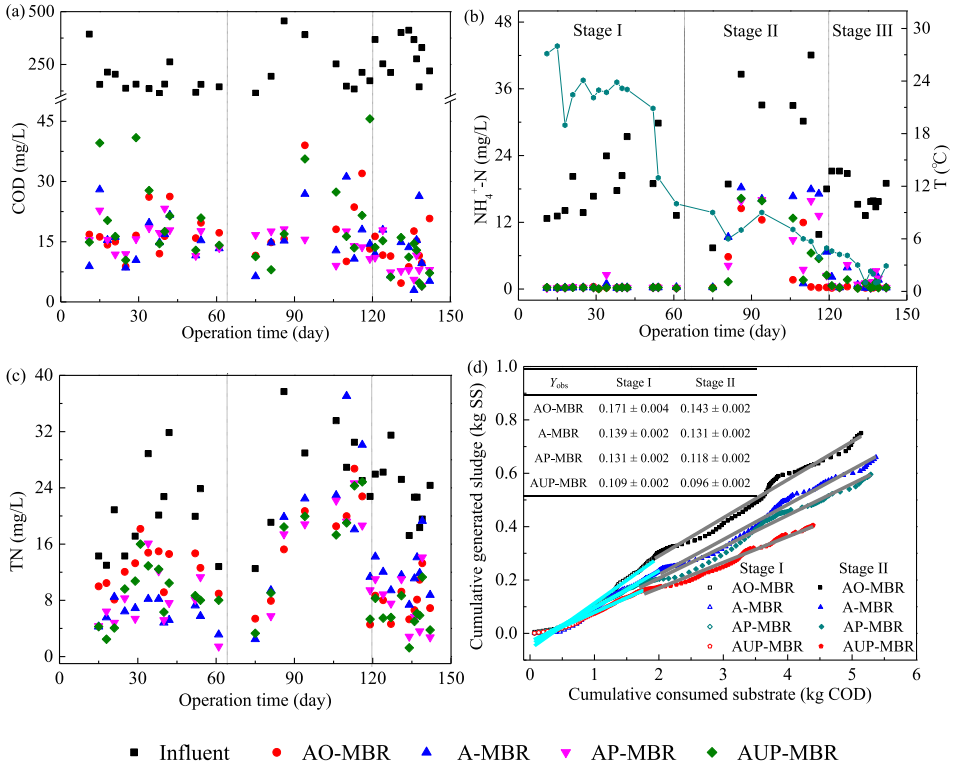

Fig. 3. COD (a), NH_4^+–N (b) and TN (c) removal and sludge accumulation (d) in the four MBRs.

stage II. TN removal was the highest in AUP-MBR (73.8%) and the lowest in A-MBR (48.8%), suggesting that ultrasonication and carriers promoted organic substrate release, which served as internal carbon sources for denitrification (Kampas et al., 2007).

3.2.2. Sludge reduction performance

As shown in Fig. 3d, applying linear regression to the curve plotting cumulative biomass production against cumulative consumed substrate leads to Y_{obs} of 0.171 and 0.143 g SS/g COD at normal temperature (stage I) and low temperature (Stage II and III) for AO-MBR. The values were much lower than the value of 0.35 g SS/g COD reported for the conventional activated sludge process (Wang et al., 2011) due to the long SRT of 108 d in AO-MBR. Meanwhile, Y_{obs} values of A-MBR, AP-MBR and AUP-MBR were 0.139, 0.131 and 0.109 g SS/g COD in Stage I, and 0.131, 0.118 and 0.096 g SS/g COD in Stage II and III, respectively. Low temperature affects microbial growth rates and microbial populations (Hulsen et al., 2016), thus resulting in lower Y_{obs} in stage II and III than that in stage I. SRE of A-MBR, AP-MBR and AUP-MBR were 18.6%, 23.4% and 36.5% at normal temperature, and decreased to 8.2%, 17.1% and 32.6% at low temperature. The results indicated that sludge reduction of A-MBR was sensitive to temperature decrease, while packing carriers and ultrasonication alleviated the deterioration and greatly improved SRE at low temperature.

3.3. Sludge reduction mechanism analysis

3.3.1. Cell lysis enhancement

Fig. 4 summarized the degree of cell breakage that occurred in each unit. The number of ruptured cells in ASSR was increased from 1.61×10^4 in $ASSR_A$ to 1.90×10^4 in $ASSR_{AP}$, and further to 2.49×10^4 cells/g SS in $ASSR_{AUP}$. It was calculated that the number of ruptured cells increased by 15.3% and 23.7% after packing carriers and ultrasonication. The ruptured cells in $ASSR_{AUP}$ were the highest since the direct contribution of UTR (20.0%) could be almost negligible if considering the dilution. It was reported that cells were damaged under anaerobic conditions while maintained their cellular structure, and bacteria lysis occurred principally under aerobic conditions (Foladori et al., 2015). Therefore, the number of ruptured cells were 1.26, 1.49, 1.68 and 1.96×10^4 cells/g SS in AO-MBR, MBR_A, MBR_{AP}, MBR_{AUP}, indicating that inserting ASSR, packing carriers and ultrasonication gradually enhanced cell lysis in the MBR system.

The calculated K_d values were 0.0328, 0.0359 and 0.0528 d^{-1} in $ASSR_A$, $ASSR_{AP}$ and $ASSR_{AUP}$, respectively, which was in the range of literature data (0.02–0.05 d^{-1}) for the stabilization process (Martínezgarcía et al., 2014). Moreover, the ORP of $ASSR_A$, $ASSR_{AP}$ and $ASSR_{AUP}$ was −32.6, −55.8 and −111.3 mV, respectively. The results confirmed that sludge endogenous decay occurred rather quickly due to a more stressful environment created by packing carrier and vulnerable structure of sludge under low-intensity ultrasound pretreatment. It was concluded that the transition from anaerobic to aerobic conditions resulted as being much more effective towards the decay of raptures cells (Foladori et al., 2015), and lower ORP in ASSR induced more cell lysis in MBR under continuous aeration.

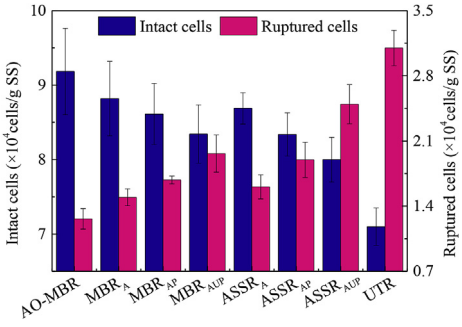

Fig. 4. Intact and ruptured cells percentage of sludge samples in four MBRs.

3.3.2. Secondary substrate release and hydrolysis

Fig. 5a showed that DOM was released in ASSRs, with SCOD in the effluent of 4.72, 9.04 and 10.82 mg/L higher than that in the influent of $ASSR_A$, $ASSR_{AP}$ and $ASSR_{AUP}$ (deducting ultrasonication release of 1.26 mg/L). Considering SCOD consumption for denitrification in ASSR (Cheng et al., 2017), the contribution of packing carriers and ultrasonication to the enhancement of SCOD release was 14.8% and 26.0%, respectively. Foladori et al. (2010) found that DOM release after ultrasonication was not due to cell membrane breakage but more probably to the solubilization of extracellular proteins and polysaccharides and increasing SCOD.

PARAFAC analysis of fluorescence spectra from four systems was conducted to further investigate DOM release and sludge hydrolysis (Fig. 5c). Component A, B and C, centered at the Ex/Em of (225, 275)/320, (235, 330)/360 and 245/450 nm, were identified as aromatic protein-like, tryptophan protein-like and humic acid-like substances, respectively (Cheng et al., 2018). As shown in Fig. 5b, FI values of refractory aromatic protein (Component A) increased by 24.52, 29.24 and 31.62 (deducted ultrasonication contribution of 7.03), while that of biodegradable tryptophan protein (Component B) decreased by 6.70, 13.71 and 24.55 from MBR to ASSR in A-MBR, AP-MBR and AUP-MBR, respectively. Compared to ASSR, packing carriers and ultrasonication enhanced FI values of Component A by 4.72 and 9.41, suggesting that ultrasonication was more conducive to refractory substrate release. The released refractory substrate was non-biodegradable in the anoxic tank and MBR, which resulted in the highest COD in the effluent of AUP-MBR (Fig. 2a). DOM release and utilization is closely related to hydrolytic and fermentative bacteria (Cheng et al., 2018a), which was major functional biomass responsible for sludge reduction. The enhanced hydrolysis of biodegradable fraction could be interpreted by more abundant secondary substance provided by ultrasonication and more diverse biomass related to sludge reduction attached on carriers.

3.3.3. Hydrolysis enhancement and uncoupling analysis

As shown in Fig. 6, protease activities of sludge in MBR_A, MBR_{AP} and MBR_{AUP} were all greatly lower than that in AO-MBR (18.7×10^{-3} U/g TS), which was related to the highest relative abundance of hydrolytic bacteria in AO-MBR. In particular, the phylum Proteobacteria, responsible for cell lysis and intracellular substances release (Cheng et al., 2018a), was enriched in AO-MBR (47.7%) and induced the production of protease. The cellular debris caused by cell lysis was mainly proteins and lipids, which could be consumed by a certain class of bacteria related to cryptic growth with low sludge yield (Lujan-Facundo et al., 2018). The protease activity of $ASSR_A$, $ASSR_{AP}$ and $ASSR_{AUP}$ was 8.23, 13.0 and 17.8×10^{-3}U/g TS, respectively, and $ASSR_{AUP}$ showed the highest protease activity. The result was coincident with DOM variations in Fig. 5. The longer SRT in $ASSR_{AP}$ and $ASSR_{AUP}$ increase the presence of bulk enzymes (Romero Pareja et al., 2015). Furthermore, significant increase of enzyme activity by packing carriers could be explained by that hydrolyzed bacteria tended to gather on packing carriers and formed thicker biofilms to resist low temperature, thus increased the protease activity to ensure utilization of macromolecular substrates. Low-strength ultrasonication has been reported to stimulate various bioprocesses, such as cell growth, enzyme synthesis and microbial fermentation (Kwiatkowska et al., 2011). Ultrasonication enhanced enzyme activity could result from

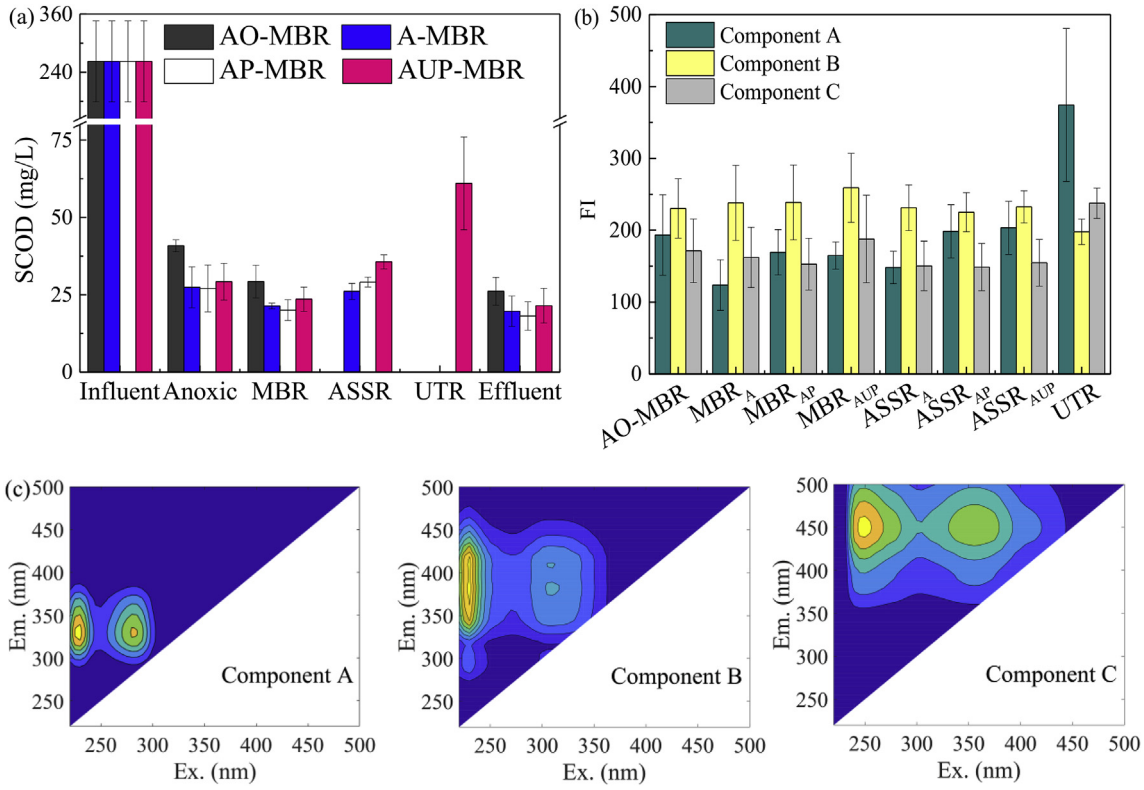

Fig. 5. DOM release and fluorescent components in four MBR-ASSRs.
(a) soluble COD, (b) peak intensity, (c) contours of three fluorescent components.

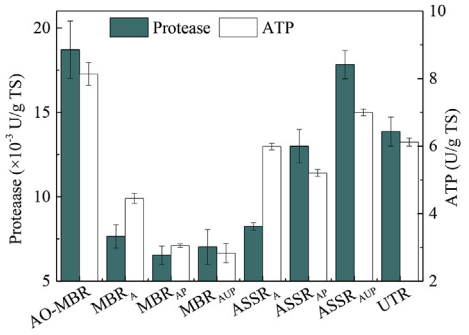

Fig. 6. Protease activity and ATP contents in the four MBR systems.

increased mass transfer due to higher specific surface area and permeability (Cho et al., 2017). The significant increase of protease activity from MBRs to corresponding ASSR was strongly associated with the release of secondary matrix in ASSRs, and the higher concentration of refractory aromatic protein in ASSR (Fig. 5b) confirmed the deduction. Furthermore, the degradation of biodegradable tryptophan protein released in ASSR was beneficial to the enhancement of protease activity. Low-intensity ultrasound and packing carriers improved the protease activity and enhanced protein hydrolysis afterwards, which contributed to sludge reduction through particle hydrolysis and lysis-cryptic growth.

The ATP content showed a significantly decreasing trend with the order of AO-MBR, MBR$_A$, MBR$_{AP}$ and MBR$_{AUP}$ (Fig. 6). Inserting ASSR decreased the ATP content in the mainstream reactors and resulted in anabolic resistance, indicated that high DO practically eliminated the ATP generation, implying a negligible anabolism activity (Ferrer-Polonio et al., 2017), and thus led to the uncoupling between anabolism and catabolism (Keskes et al., 2013). Packing carriers and ultrasonication strengthened the uncoupling effects and obtained lower sludge production. Once the sludge flowed to ASSR under lower DO, ATP production increased. The ATP contents in ASSR$_A$, ASSR$_{AP}$ and ASSR$_{AUP}$ were 5.99, 5.20 and 7.00 U/g TS, respectively. Electrons were transferred from nicotinamide adenine dinucleotide to O_2 via cytochrome and proteins bounded in cell membrane, protons are simultaneously pumped out of the cell cytoplasm. Thus a proton-motive gradient is generated across the membrane providing the driving force for the flow of protons back into the cytoplasm. ATP within the cell provides energy for a variety of cell functions. Since the carriers formed anaerobic environment and ultrasonication promoted the destruction of cell membrane, cytochrome and membrane bound proteins might be denatured, driving to a diminution of the proton gradient across cell membrane, therefore impaired electron transport capability, which decreased the ATP generation (Ferrer-Polonio et al., 2017). Decreasing ATP in the heterotrophic metabolism process available for biosynthesis would in turn reduce biomass production (Han et al., 2016).

3.4. Comparison on microbial community structures

3.4.1. Richness and diversity of bacteria

A comprehensive evaluation of the microbial community on richness and diversity of the ten sludge samples is shown in Table 2. It indicated that inserting ASSR played a key role on improving richness (Chao) and diversity (Shannon) of microbial community. Microbial communities in ASSR$_{AP}$ were richer and more diverse than in ASSR$_A$, and the richness of microbial communities in P$_{AP}$ was greatly higher than ASSR$_{AP}$ and ASSR$_A$. It was determined that packing carriers enriched biomass with long generation time and

Table 2
Richness and diversity estimators of microbial communities in AO-MBR and ASSR-MBRs ($\alpha = 0.03$).

Samples	Reads	Normalization	OTUs	Shannon	Simpson	Ace	Chao	Coverage
AO-MBR	40702	32943	887	5.36	0.0116	1047	1045	0.989
MBR_A	33414	32943	1023	5.68	0.0083	1151	1146	0.989
MBR_{AP}	40547	32943	1010	5.60	0.0089	1151	1135	0.989
MBR_{AUP}	33557	32943	995	5.56	0.0089	1149	1157	0.988
$ASSR_A$	43335	32943	1001	5.55	0.0104	1136	1149	0.989
$ASSR_{AP}$	38008	32943	1021	5.46	0.0111	1168	1190	0.987
$ASSR_{AUP}$	32943	32943	1014	5.61	0.0086	1148	1133	0.989
P_{AP}	37454	32943	1040	5.56	0.0101	1192	1193	0.988
P_{AUP}	38951	32943	1022	5.64	0.0080	1158	1164	0.989
UTR	38934	32943	1040	5.66	0.0087	1206	1203	0.988

formed longer microbial food chains, and thus enhanced microbial richness and diversity in ASSR (Cheng et al., 2018b). Compared to MBR_{AUP}, the microbial population richness and diversity in UTR was improved obviously, demonstrating that low-intensity ultrasonic technology could increase sludge microbial activity (Huan et al., 2009). Particularly, $ASSR_{AUP}$ exhibited lower richness and greater diversity than $ASSR_{AP}$. The possible cause was that low-intensity ultrasonic cavitation promoted reversible permeation, accelerated the permeability and selectivity of cell membrane and wall, and changed nutrition or molecule transport through cell membranes, thereby affected the abundance and diversity of microbial populations (Dai et al., 2003).

3.4.2. Taxonomic complexity and function of the bacterial community

Microbial community structures of four MBRs at genus level were demonstrated by a hierarchically clustered heatmap in Fig. 7. *Norank_NS9_marine_group*, *norank_Saprospiraceae* and *norank_Saccharibacteria* were the most dominant genera. The total relative abundance of *Nitrospira* and *norank_NS9_marine_group* responsible for nitrification were the highest in MBR_{AUP} (10.7%) and $ASSR_{AUP}$ (10.4%). The three major mechanisms of sludge reduction, namely hydrolysis of particulate organic matters, slow growth and lysis of bacterial biomass, are achieved by enriching hydrolytic, slow-growing and predatory bacteria in sludge reduction systems (Cheng et al., 2017; Jiang et al., 2018). The genera of bacteria responsible for sludge reduction were investigated in the four MBRs according to Fig. 7.

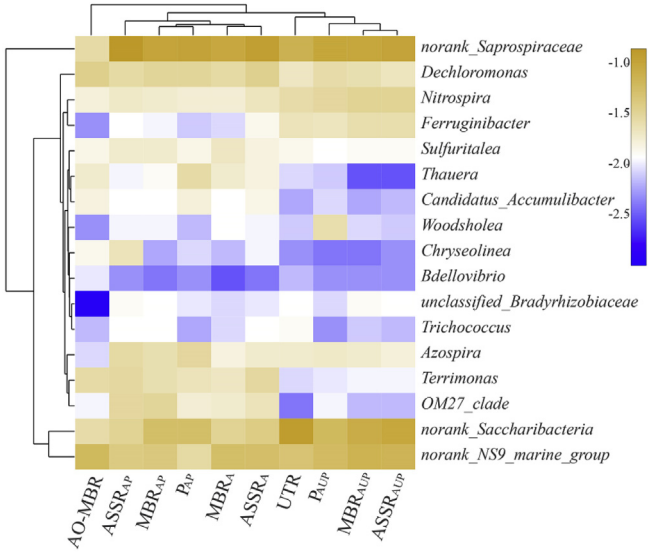

Fig. 7. Taxonomic classification of microbial communities of the four MBRs at the genus level. Relative abundance was set as the number of sequences affiliated to a given phylogenetic group divided by the total number of sequences per sample.

The relative abundance of certain kinds of hydrolytic bacteria including *norank_Saccharibacteria*, *Dechloromonas, Woodsholea* and *Ferruginibacter* was higher in ASSR-MBRs than that in the AO-MBR, which enhanced sludge reduction in ASSR-MBRs. The genus of *norank_Saccharibacteria* was greatly enriched in MBR_{AUP}, $ASSR_{AUP}$ and UTR with the relative abundance of 8.5%, 9.9% and 12.7%, respectively. Genetic studies indicated that *norank_Saccharibacteria* was a phylogenetically diverse group and played an important role in degrading various organic compounds under aerobic, nitrate-reducing and anaerobic conditions (Kindaichi et al., 2016). Carriers intensified the enrichment of *Dechloromonas* with relative abundance in P_{AP} (3.2%) and P_{AUP} (2.7%) higher than $ASSR_{AP}$ (2.9%) and $ASSR_{AUP}$ (2.2%). The relative abundance of *Woodsholea* related to hydrolysis of organic matters (He et al., 2018) was the highest in P_{AUP} of 2.6%. *Ferruginibacter* was associated with glucose fermentation (Lee et al., 2014) and preferentially enriched in MBR_{AUP} (2.6%), $ASSR_{AUP}$ (2.6%) and P_{AUP} (2.2%). Low-strength ultrasonication disintegrated sludge flocs to fine particles and soluble large molecules, and favored the growth of hydrolytic bacteria, which played important roles in hydrolysis of inactive particles.

The denitrifying bacteria *Candidatus_Accumulibacter, Dechloromonas, Thauera*, *Sulfuritalea* and *Azospira* were also classified as slow-growing bacteria with low sludge yield (Jiang et al., 2018). *Candidatus_Accumulibacter* and *Dechloromonas*, classified as denitrifying phosphorus-accumulating organisms, were preferentially enriched on the surface of carriers compared to mixed liquor. The total relative abundance of another three genera of denitrifying bacteria, *Thauera*, *Sulfuritalea* and *Azospira*, which were also classified as slow growers (Jiang et al., 2018), were the highest in $ASSR_{AP}$ (5.9%). It is indicated that ASSR-MBR by packing carriers showed higher denitrification potential and lower sludge production from the microbiological perspective. The accumulation of predatory bacteria also enhanced by packing carriers and ultrasonication with *norank_Saprospiraceae* showed the highest relative abundance in $ASSR_{AP}$ of 14.1% and *Bdellovibrio* preferentially enriched in AUP-MBR with relative abundance of 0.5%, which facilitated the lysis-cryptic growth and was partly responsible for sludge reduction in ASSR-MBRs (Cheng et al., 2017).

In this study, enhancement of sludge reduction was achieved by packing carriers and ultrasonication, especially under low temperature. Carriers provide habitat for functional bacteria responsible for hydrolysis and slow growing, create a more stressing environment with low ORP for cell lysis and hydrolysis of inactive fractions. Ultrasonication keeps cells in a vulnerable state prone to cell lysis, promotes the release of intracellular substances (Yang et al., 2012), stimulates hydrolytic enzyme excretion, and enhances uncoupling effects together with carriers in ASSR. However, ultrasonication is often not so economic to reach higher enhancement of sludge reduction (Foladori et al., 2010) because it requires

very high energy levels of 1.09 kJ/g reduced SS in AUP-MBR, which is comparable to literature of ultrasonication (Yang et al., 2015) but greatly higher than conventional sludge treatment and disposal (218–315 €/ton SS). Therefore, packing carriers is probably more cost-effective and advantageous to enhance sludge reduction by partial damage to bacterial cells and promoting better interaction between bacteria, enzymes and substrates to favor particles hydrolysis.

4. Conclusion

Effects of low temperature were negligible on COD removal, deteriorated NH_4^+–N and TN removal, and decreased SRE in ASSR-MBR. Packing carriers in ASSR and ultrasonication before ASSR both enhanced sludge reduction in ASSR-MBR, especially under low temperature. SREs of A-MBR, AP-MBR and AUP-MBR were 8.2%, 17.1% and 32.6% at 1.0–9.0 °C. Packing carriers and ultrasonication increased cell rupture by 11.1% and 14.5% in aerobic MBR, enhanced protease activity in ASSR by 60.0% and 116.3%, and reduced ATP content for heterotrophic metabolism by 31.4% and 7.3%, respectively. *MiSeq* sequencing results showed that packing carriers enriched hydrolytic bacteria (*Terrimonas, Dechloromonas* and *Woodsholea*), slow growers (*Sulfuritalea*, *Thauera* and *Azospira*) and predatory bacteria (*Bdellovibrio* and *norank_Saprospiraceae*), while ultrasonication further enriched hydrolytic bacteria (*norank_Saccharibacteria* and *Ferruginibacter*).

Acknowledgment

This work was supported by National Natural Science Foundation of China, China (51878403) and Shanghai Rising-Star Program, China (16QA1401900).

References

Arévalo, J., Ruiz, L.M., Pérez, J., Gómez, M.A., 2014. Effect of temperature on membrane bioreactor performance working with high hydraulic and sludge retention time. Biochem. Eng. J. 88, 42–49.
Cheng, C., Zhou, Z., Niu, T.H., An, Y., Shen, X.L., Pan, W., Chen, Z.H., Liu, J., 2017. Effects of side-stream ratio on sludge reduction and microbial structures of anaerobic side-stream reactor coupled membrane bioreactors. Bioresour. Technol. 234, 380–388.
Cheng, C., Zhou, Z., Pang, H., Zheng, Y., Chen, L., Jiang, L.M., Zhao, X., 2018a. Correlation of microbial community structure with pollutants removal, sludge reduction and sludge characteristics in micro-aerobic side-stream reactor coupled membrane bioreactors under different hydraulic retention times. Bioresour. Technol. 260, 177–185.
Cheng, C., Zhou, Z., Qiu, Z., Yang, J., Wu, W., Pang, H., 2018b. Enhancement of sludge reduction by ultrasonic pretreatment and packing carriers in the anaerobic side-stream reactor: performance, sludge characteristics and microbial community structure. Bioresour. Technol. 249, 298–306.
Cho, S.K., Yun, Y.M., Shin, S.G., 2017. Low-strength ultrasonication positively affects methanogenic granules toward higher AD performance: hydrolytic enzyme excretions. Ultrason. Sonochem. 36, 168–172.
Dai, C., Wang, B., Duan, C., Sakanishi, A., 2003. Low ultrasonic stimulates fermentation of riboflavin producing strain *Ecemothecium ashbyii*. Colloids Surf., B 30 (1–2), 37–41.
Ferrer-Polonio, E., Fernandez-Navarro, J., Alonso-Molina, J.L., Amoros-Munoz, I., Bes-Pia, A., Mendoza-Roca, J.A., 2017. Changes in the process performance, sludge production and microbial activity in an activated sludge reactor with addition of a metabolic uncoupler under different operating conditions. J. Environ. Manag. 203 (Pt 1), 349–357.
Foladori, P., Tamburini, S., Bruni, L., 2010. Bacteria permeabilization and disruption caused by sludge reduction technologies evaluated by flow cytometry. Water Res. 44 (17), 4888–4899.
Foladori, P., Velho, V.F., Costa, R.H., Bruni, L., Quaranta, A., Andreottola, G., 2015. Concerning the role of cell lysis-cryptic growth in anaerobic side-stream reactors: the single-cell analysis of viable, dead and lysed bacteria. Water Res. 74, 132–142.
Han, X., Wang, Z., Wang, X., Zheng, X., Ma, J., Wu, Z., 2016. Microbial responses to membrane cleaning using sodium hypochlorite in membrane bioreactors: cell integrity, key enzymes and intracellular reactive oxygen species. Water Res. 88, 293–300.
Han, X., Wang, Z., Chen, M., Zhang, X., Tang, C.Y., Wu, Z., 2017. Acute responses of microorganisms from membrane bioreactors in the presence of NaOCl: protective mechanisms of extracellular polymeric substances. Environ. Sci. Technol. 51 (6), 3233–3241.
He, Q., Song, Q., Zhang, S., Zhang, W., Wang, H., 2018. Simultaneous nitrification, denitrification and phosphorus removal in an aerobic granular sequencing batch reactor with mixed carbon sources: reactor performance, extracellular polymeric substances and microbial successions. Chem. Eng. J. 331, 841–849.
Hoang, V., Delatolla, R., Abujamel, T., Mottawea, W., Gadbois, A., Laflamme, E., Stintzi, A., 2014. Nitrifying moving bed biofilm reactor (MBBR) biofilm and biomass response to long term exposure to 1 °C. Water Res. 49, 215–224.
Huan, L., Yiying, J., Mahar, R.B., Zhiyu, W., Yongfeng, N., 2009. Effects of ultrasonic disintegration on sludge microbial activity and dewaterability. J. Hazard Mater. 161 (2–3), 1421–1426.
Hulsen, T., Barry, E.M., Lu, Y., Puyol, D., Batstone, D.J., 2016. Low temperature treatment of domestic wastewater by purple phototrophic bacteria: performance, activity, and community. Water Res. 100, 537–545.
Jiang, L.M., Zhou, Z., Niu, T., Jiang, L., Chen, G., Pang, H., Zhao, X., Qiu, Z., 2018. Effects of hydraulic retention time on process performance of anaerobic side-stream reactor coupled membrane bioreactors: kinetic model, sludge reduction mechanism and microbial community structures. Bioresour. Technol. 267, 218–226.
Kampas, P., Parsons, S.A., Pearce, P., Ledoux, S., Vale, P., Churchley, J., Cartmell, E., 2007. Mechanical sludge disintegration for the production of carbon source for biological nutrient removal. Water Res. 41 (8), 1734–1742.
Keskes, S., Bouallagui, H., Godon, J.J., Abid, S., Hamdi, M., 2013. Biological sludge reduction during abattoir wastewater treatment process using a sequencing batch aerobic system. Environ. Technol. 34 (1–4), 333–341.
Kindaichi, T., Yamaoka, S., Uehara, R., Ozaki, N., Ohashi, A., Albertsen, M., Nielsen, P.H., Nielsen, J.L., 2016. Phylogenetic diversity and ecophysiology of Candidate phylum Saccharibacteria in activated sludge. FEMS Microbiol. Ecol. 92 (6), 11.
Kwiatkowska, B., Bennett, J., Akunna, J., Walker, G., Bremner, D., 2011. Stimulation of bioprocesses by ultrasound. Biotechnol. Adv. 29 (6), 768–780.
Lee, B.I., Kang, H., Kim, H., Joung, Y., Joh, K., 2014. Ferruginibacter yonginensis sp. nov., isolated from a mesotrophic artificial lake. Int. J. Syst. Evol. Microbiol. 64 (Pt 3), 846–850.
Lujan-Facundo, M.J., Fernandez-Navarro, J., Alonso-Molina, J.L., Amoros-Munoz, I., Moreno, Y., Mendoza-Roca, J.A., Pastor-Alcaniz, L., 2018. The role of salinity on the changes of the biomass characteristics and on the performance of an OMBR treating tannery wastewater. Water Res. 142, 129–137.
Martínezgarcía, C.G., Olguín, M.T., Fall, C., 2014. Aerobic stabilization of biological sludge characterized by an extremely low decay rate: modeling, identifiability analysis and parameter estimation. Bioresour. Technol. 166 (8), 112–119.
Niu, T., Zhou, Z., Ren, W., Jiang, L.M., Li, B., Wei, H., Li, J., Wang, L., 2016a. Effects of potassium peroxymonosulfate on disintegration of waste sludge and properties of extracellular polymeric substances. Int. Biodeterior. Biodegrad. 106, 170–177.
Niu, T., Zhou, Z., Shen, X., Qiao, W., Jiang, L.M., Pan, W., Zhou, J., 2016b. Effects of dissolved oxygen on performance and microbial community structure in a micro-aerobic hydrolysis sludge in situ reduction process. Water Res. 90, 369–377.
Pang, H., Zhou, Z., Niu, T., Jiang, L.-M., Chen, G., Xu, B., Jiang, L., Qiu, Z., 2018. Sludge reduction and microbial structures of aerobic, micro-aerobic and anaerobic side-stream reactor coupled membrane bioreactors. Bioresour. Technol. 268, 36–44.
Romero-Pareja, P.M., Aragon, C.A., Quiroga, J.M., Coello, M.D., 2017. Evaluation of a biological wastewater treatment system combining an OSA process with ultrasound for sludge reduction. Ultrason. Sonochem. 36, 336–342.
Romero Pareja, P.M., Real Jiménez, A., Aragón, C.A., Quiroga, J.M., Coello, M.D., 2015. Changes in enzymatic and microbiological activity during adaptation of a conventional activated sludge (CAS) to a CAS-oxic-settling-anaerobic (OSA) adapted process. Desalin. Water. Treat. 57 (6), 2719–2725.
Saby, S., Djafer, M., Chen, G.H., 2003. Effect of low ORP in anoxic sludge zone on excess sludge production in oxic-settling-anoxic activated sludge process. Water Res. 37 (1), 11–20.
Semblante, G.U., Hai, F.I., Bustamante, H., Price, W.E., Nghiem, L.D., 2016. Effects of sludge retention time on oxic-settling-anoxic process performance: biosolids reduction and dewatering properties. Bioresour. Technol. 218, 1187–1194.
Sepehri, A., Sarrafzadeh, M.-H., 2018. Effect of nitrifiers community on fouling mitigation and nitrification efficiency in a membrane bioreactor. Chemical Engineering and Processing - Process Intensification 128, 10–18.
Troiani, C., Eusebi, A.L., Battistoni, P., 2011. Excess sludge reduction by biological way: from experimental experience to a real full scale application. Bioresour. Technol. 102 (22), 10352–10358.
Van de Moortel, N., Van den Broeck, R., Degreve, J., Dewil, R., 2017. Comparing glow discharge plasma and ultrasound treatment for improving aerobic respiration of activated sludge. Water Res. 122, 207–215.
Velho, V.F., Foladori, P., Andreottola, G., Costa, R.H.R., 2016. Anaerobic side-stream reactor for excess sludge reduction: 5-year management of a full-scale plant. J. Environ. Manag. 177, 223–230.
Wang, J., Li, S.Y., Jiang, F., Wu, K., Liu, G.L., Lu, H., Chen, G.H., 2015. A modified oxic-settling-anaerobic activated sludge process using gravity thickening for excess sludge reduction. Sci. Rep. 5, 13972.
Wang, Q., Wang, Z., Wu, Z., Han, X., 2011. Sludge reduction and process performance in a submerged membrane bioreactor with aquatic worms. Chem. Eng. J. 172 (2), 929–935.

Xie, B., Liu, H., Yan, Y., 2009. Improvement of the activity of anaerobic sludge by low-intensity ultrasound. J. Environ. Manag. 90 (1), 260–264.
Yang, S.-S., Guo, W.-Q., Cao, G.-L., Zheng, H.-S., Ren, N.-Q., 2012. Simultaneous waste activated sludge disintegration and biological hydrogen production using an ozone/ultrasound pretreatment. Bioresour. Technol. 124 (0), 347–354.
Yang, S.-S., Guo, W.-Q., Chen, Y.-D., Wu, Q.-L., Luo, H.-C., Peng, S.-M., Zheng, H.-S., Feng, X.-C., Zhou, X., Ren, N.-Q., 2015. Economical evaluation of sludge reduction and characterization of effluent organic matter in an alternating aeration activated sludge system combining ozone/ultrasound pretreatment. Bioresour. Technol. 177, 194–203.
Ye, F.-X., Zhu, R.-F., Li, Y., 2008. Effect of sludge retention time in sludge holding tank on excess sludge production in the oxic-settling-anoxic (OSA) activated sludge process. J. Chem. Technol. Biotechnol. 83 (1), 109–114.
Zhou, Z., Qiao, W., Xing, C., An, Y., Shen, X., Ren, W., Jiang, L.-m., Wang, L., 2015. Microbial community structure of anoxic–oxic-settling-anaerobic sludge reduction process revealed by 454-pyrosequencing. Chem. Eng. J. 266, 249–257.